Doping-Induced Structural Changes of Conducting Polyalkoxythiophene on the Chemically Modified Gold Surface: An in Situ Surface Enhanced Resonance Raman Spectroscopic Study

Natalia Kocharova,* Jukka Lukkari, Antti Viinikanoja, Timo Ääritalo, and Jouko Kankare

Department of Chemistry, University of Turku, FIN-200014 Turku, Finland

Received: June 7, 2002; In Final Form: August 13, 2002

In situ surface enhanced resonance Raman spectroscopy (SERRS) with excitation at 1064 nm has been used to monitor the dynamic changes in charge transfer, structure, and orientation during the redox doping of a self-assembled monolayer of conducting poly-3-(3′-thienyloxy)propanesulfonate (P3TOPS) on a gold surface modified by 2-mercaptoethylamine (MEA). The SERRS spectra were compared with Fourier transform Raman spectra of solid 3TOPS monomer and with reduced and oxidized forms of P3TOPS in solution. The oxidative doping of P3TOPS has been carried out in the potential range between −0.3 and +0.7 V, vs Ag/AgCl. Our SERRS data indicate that the oxidation process goes through initial preferential generation of polaron charge carriers with followed generation of bipolarons at higher oxidation levels. At low doping levels, thiophene rings are more coplanar than at higher ones. The observed potential dependence of the normalized integrated SERRS intensities of P3TOPS in the range of the inter-ring stretch vibrations exhibits a bell-shaped curve with a maximum at 0 V. In the potential window from −0.1 to +0.1 V, the highest number of doped coplanar neighboring molecular units is achieved. Reorientation of alkoxy side chain closer to the surface normal starts at −0.1 V. At higher potentials applied, the trans → gauche conformational transformation of the alkoxy side chain was observed along with the massive growing number of bipolarons and simultaneous deplanarization of the polymer chain.

1. Introduction

Conjugated polythiophene (PT) derivatives have attracted much attention because of semiconducting properties based on their conjugation length change, which can be controlled by chemical or electrochemical doping.[1,2] A recently developed technique of molecular self-assembly of nanoscale multicomposite films by layering of oppositely charged ionic macromolecular compounds has become a rapidly developing method for creating of conducting polyelectrolyte multilayers (PEMs).[3−11] The side chains of PT derivatives in PEMs can act as arms for directed self-assembly of the polymer.[1] However, the main drawback of PT derivatives is the instability of their conductive form. Poly-3-(3′-thienyloxy)-1-propanesulfonate (P3TOPS) is one example of semiconducting conjugated polyelectrolyte[12−15] where these disadvantages seemingly obviated. Indeed, sulfonic acid substitution in the P3TOPS side chain increases water solubility and gives the polymer a self-doping character.[16] Alkoxy group attached to the 3 position of thiophene ring protects it from undesired oxidation processes, lowers the oxidation potential, and stabilizes the conducting state of the polymer.[1] We have recently shown[14] that P3TOPS can be used as a polyanion in PEM preparation and that its oxidation state affects the multilayer formation. Also, by measuring the charge-transfer rate across an insulating polyelectrolyte between the substrate and the P3TOPS layer with electromodulated reflectance, it has been shown[15] that the charge-transfer rate can be regarded as a measure of interpenetrating of the P3TOPS layer toward the electrode surface.

Conductivity of polythiophenes directly depends on their cristallinity, extent of planarity,[17] face-to-face interchain stacking,[18] and a proper chemical modification of the molecular unit.[19] The difference in conductivity upon doping observed experimentally among PT, polypyrrole, polyfurane, and polyselenophene was attributed not only to differences in HOMO and LUMO bandwidths and their band gaps[20] but mainly to disorder and crystal packing effects.[21] For example, the interchain coupling existing in self-assembled regioregular poly(3-hexylthiophene) films drastically changes the properties of self-localized polaron excitations leading to the appearance of multiple absorption bands.[22,23] In earlier works by Kawai et al.,[24,25] it has been also shown that in case of poly(3-alkylthiophene)s the existence of side chains not in the all-trans conformation results in increase of the lattice parameter *b*. The precise role of alkoxy side chains in the conductivity is still not clear, as well as details concerning structure/property interrelationships of polyalkoxythiophenes are still incomplete.

The lack of in situ spectroscopic information about structural changes of self-assembled polyalkoxythiophenes upon electrochemical doping prompted us to investigate the Fourier transform (FT) resonance Raman (RR) spectra of P3TOPS and surface-enhanced resonance Raman scattering (SERRS) spectra of its monolayer. The main issues we focus on in this work are structural evolution and orientational behavior of a conducting P3TOPS layer adsorbed on a chemically modified gold electrode. Accordingly, the following questions about structural evolution of P3TOPS monolayer on Au/MEA surface can be posed: (1) in what potential window is the highest conjugation length of P3TOPS achieved? (2) How does it correlate with

* To whom correspondence should be addressed. Phone: +358-2-3336713. Fax: +358-2-3336700. E-mail: natkot@utu.fi.

10.1021/jp026259g CCC: $22.00
Published on Web 09/26/2002

thiophene ring structural changes in P3TOPS? (3) Does the conformational change in the side chain occur upon doping, and how does it correlate with the conjugation length of the oxidized polymer?

Large surface enhancements in SE(R)RS, according to the predictions of the electromagnetic (EM) theory, are not restricted to species in direct contact with the SERS-active metal surface but also occur for nanometer-scale molecule−metal separations.[26−32] Recent progress in the overlayer SERS technique has been exhaustively reviewed by Weaver et al.[26] Generally, with use of spacers such as alkyl chains, Raman intensity decays within overlayer thickness, $d \leq 2-3$ nm,[33,34] giving largest SER enhancement closer to gold substrate, say $d \leq 1$ nm.[26] Taking into consideration that in the SERRS study described herein the length of the mercaptoethylamine (MEA) molecule used as a dielectric surface modifier is approximately 4 Å, a large EM enhancement is therefore expected.

2. Experimental Section

2.1. Materials and Sample Preparation Methods. Aminoethanethiol hydrochloride (MEA) as well as the chemicals needed for the synthesis of sodium 3-(3′-thienyloxy)propanesulfonate have been purchased from Aldrich and used as received. P3TOPS was prepared following the procedures described previously.[35,14,15] The working electrode was a polycrystalline 2 mm diameter gold rod mounted in Teflon holder from CH Instruments (Texas). The counter electrode was a platinum wire, and a saturated calomel electrode (SCE) was used as a reference electrode.

Because reproducible formation and stability of the monolayer systems and, therefore, SER(R)S spectra quality are very dependent on the pretreatment of gold surface, special attention was paid to the gold surface preparation. Electrochemical pretreatment of the gold electrode was performed as follows. The gold electrode was polished to a mirror finish with progressively finer grades of alumina, ending with 0.1 μm grade. The electrode was then rinsed with Millipore water (18 MΩ) and cleaned by oxidation−reduction cycles vs $Hg/HgSO_4$ in 0.5 M sulfuric acid. Finally, according to the well-known procedure,[36] electrochemical roughening of the electrode in 0.1 M KCl solution was performed. A total of 30 voltammetric cycles yielded a surface with a roughness factor of 5.1, which is sufficient for obtaining stable and intense SERS spectra.

Primary modification of the Au electrode surface with positively charged ammonium groups was performed by soaking the electrode in aqueous 1 mM solution of MEA for 1 h, followed by rinsing with Millipore water.[14,15] The P3TOPS layer was deposited onto the MEA-modified electrode from aqueous 0.001 M (with respect to monomer) solution of oxidized P3TOPS. The ionic strength was adjusted by Na_2SO_4 to 0.02 M.

2.2. Instrumental and Experimental Configuration. P3TOPS was characterized in solution by UV−vis spectroscopy using a Hewlett-Packard 8453 spectrophotometer. FT RR and SERRS spectra were recorded on a Nicolet (model Nexus 870) FT-IR spectrometer equipped with FT Raman module. Nd:YAG near-infrared laser ($\lambda_{ex} = 1064$ nm) and a Ge detector operated at liquid-nitrogen temperature were in use. SERRS measurements were carried out in a homemade single-compartment 3-electrode spectro-electrochemical cell with glass window. As an electrolyte, a 0.2 M NaF solution bubbled by argon was used. All of the measurements were made using a 180° backscattering geometry and with spectral resolution set at 4 cm^{-1}. The Raman spectrum of solid monomer 3TOPS and RR spectra of liquid polymer P3TOPS were obtained in suitable sealed capillary tubes. The laser power was kept on levels of 43 and 27 mW for normal FT-Raman and SERRS measurements, respectively. In all Raman and SERRS experiments, 1000 scans were collected to improve the signal-to-noise ratio. A background spectrum of MEA at an open circuit potential was subtracted from each spectrum in order to remove the alkanethiol contributions and to show only the P3TOPS response and its dependence on applied potential. Deconvolution of the spectra was carried out using the Microcal Software Inc. ORIGIN 6.0 program.

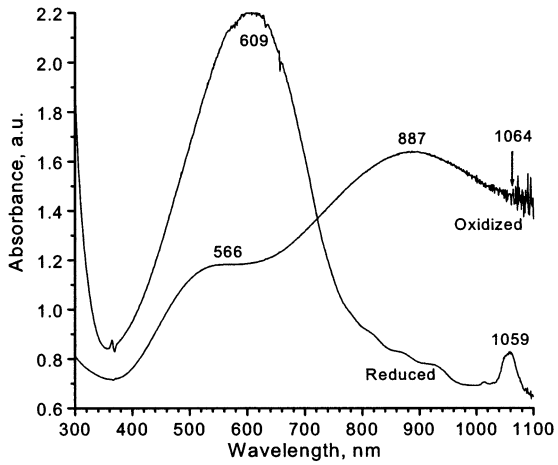

Figure 1. UV−vis spectra of P3TOPS (mw = 3700, number of units is about 17) in 0.1 M $NaNO_3$ at oxidized and reduced state. The arrow indicates Nd:YAG laser excitation line.

3. Results and Discussion

3.1. Optical Characterization of the Polymer. In air, P3TOPS exists in the oxidized form. Reduction of P3TOPS was performed by hydrazine monohydrate. The UV/vis spectra of reduced and oxidized forms of P3TOPS in water are presented in Figure 1. The line at 1059 nm comes from hydrazine monohydrate. The $\pi \rightarrow \pi\pi^*$ transition at 609 nm of the reduced P3TOPS is broad and does not show any resolvable vibronic fine splitting. This fact indicates a wide range of conformations[37,4] and reflects a twisting of polymer backbone.

The oxidized form of P3TOPS displays a blue shift of the 609 nm (2.0 eV) absorption band to 566 nm (2.2 eV), and a new wide band is formed with a maximum at 887 nm (1.4 eV). The blue shift can be attributed to shortening of $\pi-\pi$ conjugation by partial deplanarization of chain fragments.[38]

3.2. Raman Spectrum of 3TOPS. In Figure 2 are shown the Raman spectra of solid monomer 3TOPS and the reduced and oxidized forms of the polymer P3TOPS in aqueous solution in the range of 1600−350 cm^{-1}. Strong normal vibrations of the thiophene ring dominate in the Raman spectra of 3TOPS and P3TOPS. Raman spectrum of 3TOPS is typical for thiophene[39] except for the additional alkoxy group bands.

The complete reliable assignments of the vibrational spectra of neutral polyalkoxythiophenes have not been obtained yet, although a multitude of normal coordinate calculations and experimental infrared and Raman measurements for neutral thiophene (T),[39,40] PT,[41−49] polyalkylthiophenes,[47−49] and polyalkoxythiophenes[12,50−52] has been carried out.

The assignment of the observed Raman bands of 3TOPS have been made based on the available literature data and presented in Table 1. Comparison of the Raman spectrum of 3TOPS with that of the model compound 3-methoxypropane-1-sulfonate containing an ether group (not shown) leads to the assignment of the band at 1473 cm^{-1} to a mode containing symmetric ring

TABLE 1: Summary of Major Raman Modes of Poly-3-(3′-thienyloxy)-1-propanesulfonate (in cm^{-1})

	resonance Raman		SERRS	
3TOPS	P3TOPS	P3TOPS$_{ox}$	P3TOPS/Au	mode description[a]
	1523	1515−1540	1503−1570	$\nu_{as}(C_\alpha{=}C_\beta)$
1473	1442		1450	$\nu_s(C_\alpha{=}C_\beta) + \delta(0CH)$
1424, 1406	1393	1424, 1393, 1397	1396−1463	$\nu_s(C_\alpha{=}C_\beta)$
1302	1365	1365	1290−1371	$\nu_s(C_\beta{-}C_\beta)$
871	920	920	912−918	ν(CSC)
	1202	1202	1202	$\nu_{as}(C_\alpha{-}C_{\alpha'})$
	1212	1212, 1228	1212,1228, 1232	$\nu_s(C_\alpha{-}C_{\alpha'})$
970	1093	1093	1107	ν_{as}(COCC)
1062	1062	1062	1068	$\nu_{as}(C{-}O{-}C)_{gauche}$
829			860	ν_s(CSC) + $\nu_s(C_\beta{-}O{-}O)$
752	711	711	706, 721, 744	$\delta(CSC)_{ring}$
1244	1247	1247	1258−1265, 1245−1253	$\nu(C_\alpha{-}C_{\alpha'}) + \delta(C_\beta H)$
1035		1040, 1053	1037	$\delta(C_\beta H)$
1071	1080	1086−1093	1082	$\delta(C_\beta O) + \delta(C_\beta H)$
	1014	1008	1007	$\nu_{as}(C_\beta{-}O)$
913−903		698	645, 682−701, 906−908	$\gamma(C_\beta H)$
			480−485	δ(COC)
457	417	417	420−430	$\delta(C_\beta{-}O{-}C{-}C{-}C)$
280			280−295	$\delta(C_\beta{-}O)$

[a] ν_s, symmetric stretch; ν_{as}, antisymmetric stretch; δ, in-plane deformation; γ, out-of-plane deformation.

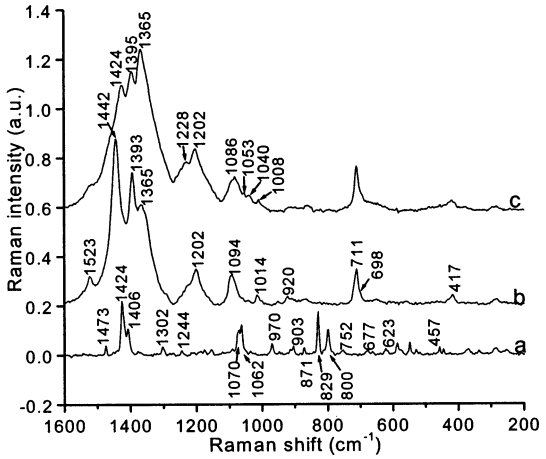

Figure 2. FT resonance Raman spectra of (a) solid monomer 3-(3′-thienylloxy)-1-propanesulfonate (3TOPS) and the reduced (b) and oxidized (c) forms of the 0.01 mM P3TOPS aqueous solution in the 1600−200 cm^{-1} spectral region.

($C_\alpha{=}C_\beta$) stretch coupled with in-plane bend of methylene group attached to oxygen.

Other observed bands are due to the side chain. The band at 1062 cm^{-1} is usually attributed to the gauche conformation of the C−O−C group.[39,53] (COC) symmetric deformation lies at 457 cm^{-1}. Asymmetrical stretch of the C_β−O bond locates at 970 cm^{-1}. The bands at 623 and 550 cm^{-1} can be attributed to the deformations of the ($-SO_3$) group.[55] Weak bands at 370 and 340 cm^{-1} most likely come from in- and out-of-plane deformations in the ($-C-SO_3$) linkage, respectively.

3.3. Change in Molecular Symmetry. It is known that strong steric interactions and torsions of the side chains due to thermal or solvent effects produce changes in molecular planarity, with corresponding changes in the symmetry of the molecule. Thus, bithiophene (α-2T) belongs to the C_{2h} point group, thiophene and terthiophene (α-3T) belong to the C_{2v} point group, and polythiophene belongs to the D_{2h} point group; in principle, planar molecules α-2T, α-4T, α-6T belong to the molecular point group C_{2h}.[40] The main effect on the frequencies and intensities in the RR and SERRS spectra depends on the changes in the delocalization of the π electrons. In polar solvents, solvent molecules can facilitate and stabilize the molecular twist. If twisting of thiophene rings takes place, π-electron localization increases, which destroys the perfect symmetry of the ion, and with the corresponding vibrational potential change, the symmetry changes to the C_2 structure.[41] Possible torsions around the C−C bond linking the alkyl- or alkoxy-group to the thiophene ring,[16,57−59] repulsions and Coulomb interactions[60,61] within the molecule, oxidation and overoxidation processes of polymer also generate disorder in the molecular chain[49] and change the molecular symmetry from C_{2v} through C_{2h} and D_{2h} to C_s. This should certainly be reflected in Raman spectra.

3.4. Raman Spectra of P3TOPS. Raman spectra were obtained from aqueous polymer solutions that were 10 mM with respect to the monomers. The reduced state of P3TOPS was obtained by reduction of the self-doped polymer by hydrazine monohydrate (Figure 2b). Very intensive bands at 1442 and 1365 cm^{-1} in RR spectrum of the reduced polymer are assigned to the C_{2h} (planar bithiophene) normal modes[46,62−64] of the ($C_\alpha{=}C_\beta$) bond in bulk thiophene rings[56] and ($C_\beta{-}C_\beta$) bond, respectively.

Generally speaking, two effects influence independently the planarity and conjugation length in the neutral state, namely, chemical substitution and the polarity of the solvent. Chemical substitution *directly* does not effect the main π-electron system,[65] and although electron donor properties of methoxy groups increase the electronic conjugation favoring coplanarization between thiophene rings,[37] steric hindrance created by the methoxy groups acts in the opposite direction favoring a twisted structure. The state of disorder established by the doping process greatly depends on the type of the solvent in which the polymer was dissolved.[49]

Careful examination of the band at the vicinity of 1393−1397 cm^{-1} reveals two overlapping vibrational modes (not shown), which become clearer in SERRS. Both of them can be assigned to the quinoid structure[56] of the ($C_\alpha{-}C_\beta$)−H bond. It is interesting that Lefrant et al have observed this band in the in situ RR spectra of oxidized poly(3,3′-dibutoxy-2,2′-bithiophene)[51] and poly(3,4-ethylenedioxythiophene).[56] They reported about a wavenumber shift upon electrochemical doping for normal symmetric ($C_\alpha{=}C_\beta$)−H vibration: 1449,[51] 1423[56] cm^{-1} → 1410 cm^{-1} (semi-quinoid structure) → 1450 cm^{-1} (quinoid structure). Furukawa[46] observed quinoid polaronic structure of the ($C_\alpha{-}C_\beta$)−H bond in the RR spectra of α-sexithiophene at 1405 cm^{-1}. The second band at higher frequency (maximum at

1397 cm^{-1}) becomes more intense in the RR spectrum of the oxidized P3TOPS. We tend to believe that it belongs to the symmetric stretch vibration of polaronic ($C_\alpha-C_\beta$)−H bond with higher positive charge. In contrast to the $C_\beta-C_\beta$ bond,[55] the $C_\alpha=C_\beta$ linkage in regiorandom polythiophene is very sensitive not only to the doping level of the polymer[51,55,66] but also to the local charge within a ring. The existence of localized charge at the $C_\alpha=C_\beta$ linkage is also confirmed by high intensity of the normal 1442 cm^{-1} mode, because the RR intensities reflect structural differences between the electronic ground and excited states:[46] the greater the difference, the more intensive a line is observed. Three vibrational modes at 1442, 1365, and 1393 cm^{-1} are typical for benzenoid-structured polythiophenes[41−44,49,56,67,68] and show twisted character of the P3TOPS molecule in aqueous medium.

Other bands observed in the Raman spectra of reduced P3TOPS are listed in Table 1. The mode at 1014 cm^{-1} is the asymmetric C_β−O stretch,[39] and the bands at 920 and 711 cm^{-1} are the CSC stretch and the intra-ring CSC deformation, respectively. A weak band at 417 cm^{-1} is the COC symmetric deformation in the side chain.[39] The shoulder at 698 cm^{-1} has been assigned[39,40,44] to the distorted part of the thiophene ring (one of the kink modes).

It is known[2] that the formation of polarons (radical-cations) and bipolarons (radical-dications) by charges injected to the conjugated backbone (oxidative doping) induces a strong modification in the electronic structure of the polymer, and new subgap optical transitions give rise to three features in the absorption spectra. For example, calculated UV−vis spectra for α-6T[2], which are consisted with most of the experimental absorption data on doped thiophene derivatives, show three electronic transitions: two for polarons at 1.2 and 1.5 eV and one transition for bipolaron at 1.1 eV. The use in resonance Raman and SERRS experiments of near-IR excitation line at 1064 nm (1.17 eV) suggests that it is in resonance with both polarons and bipolarons charge carriers although greater enhancement of bipolaron excitations is expected. Doping induced distributed charges within a polymer molecule cause an induced electric dipole moment, make it highly polarized, and initiate very strong vibrational activity to originally silent modes in the pristine polymer.

Now we turn to the RR spectrum of oxidized P3TOPS (Figure 2c). The most noticeable difference between the RR spectra of oxidized and reduced forms of P3TOPS is observed in the 1600−1300 cm^{-1} region, where the sharp and intense ($C_\alpha=C_\beta$)−H normal mode belonging to the C_{2h} point group (bulk thiophene rings[56]) at 1442 cm^{-1} decreases. On the other hand, the band belonging to the C_{2v} point group at 1424 cm^{-1} becomes more enhanced because of the increased coplanarization between the molecular units (bithiophene → terthiophene) in P3TOPS. A small shoulder at 1442 cm^{-1} implies the presence of undoped fragments. Simultaneously, we observe the enhancement of the bipolaron band at 1397 cm^{-1}. A strong enhancement of the normal intra-ring ($C_\beta-C_\beta$) mode at 1365 cm^{-1}, coming from neutral species, is also observed in the RR spectrum of oxidized P3TOPS (perhaps because of the partly twisted structure of the main chain in polar water solvent).

Splitting of the sharp normal mode at 1523 cm^{-1} of ($C_\alpha-C_\beta$) asymmetric stretch vibration in the RR spectrum of reduced P3TOPS into the multiple bands of the oxidized compound confirms the generation of quinoid-like differently conjugated fragments. The combined intensities of these bands in the RR spectrum of oxidized P3TOPS are approximately equal to the intensity of the initial 1523 cm^{-1} band which indicates that this vibration undergoes a frequency splitting because of the structural isomerism.

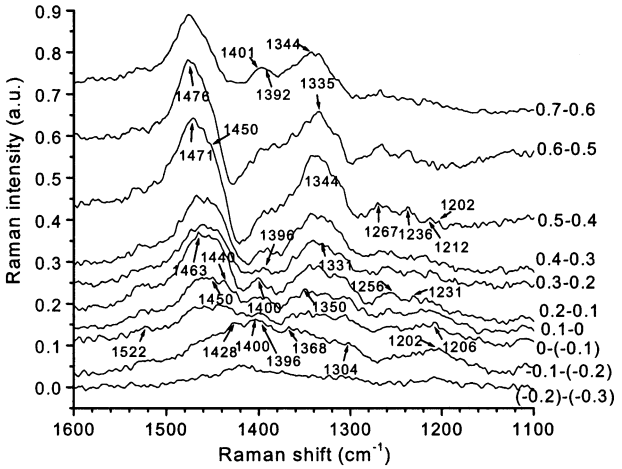

Figure 3. Differential SERRS of P3TOPS deposited from 0.01 M solution in 0.02 M Na_2SO_4 on MEA modified Au electrode in electrochemical cell filled with 0.2 M NaF solution. Excitation line 1064 nm.

3.5. SERRS Spectra of P3TOPS. Before considering in situ SERRS spectra, some specific characteristics of the SER(R)S phenomenon should be recalled. First of all, Raman selection rules do not work in SER(R)S, which results in the appearance of normally forbidden Raman modes. Overtone and combination bands are not prevalent. Vibrational band frequencies as well as SER(R)S intensities depend on the applied electrode potential in electrochemical experiment, and the dependence is different for different sets of vibrational modes. Now we turn to the SERRS results obtained in situ during the electrochemical oxidation of a P3TOPS monolayer adsorbed on MEA modified gold surface in potential range from −0.3 to +0.7 V.

3.5.1. Doping-Induced Bands in the SERRS Spectra of P3TOPS. The SERRS bands present in the 1600−1130 cm^{-1} region of inter- and intraring stretch vibrations are very intense because of strong coupling between the charge carriers and the normal vibrational modes. Because of the large number of vibrational modes present in this region and their overlap with each other, we sometimes had difficulties in making proper assignments. Therefore, to improve the reliability of the peak positions, each spectrum was subtracted from the previous one after initial normalization to yield data in the form of difference spectra. In addition, the curve fitting with the same set of pure Lorentzian lines was applied to each original SERRS spectrum.

The differential and some of the deconvoluted SERRS spectra are presented in Figures 3 and 4, respectively. A peculiarity of SE(R)RS spectra is a simultaneous existence of split Raman bands belonging to the same vibration of different molecular symmetries. Different conformations and a strong electromagnetic field at the gold−film interface cause changes in dipole moment vectors in the polarizability matrix that leads to the appearance of bands of the same origin but of different energy reflecting in SERRS spectra. Therefore, the simultaneous presence of polaron- and bipolaron bands corresponding to different conjugation bond lengths, as well as normal vibrational modes which are not allowed in simple Raman and RR spectroscopy, is not surprising in the SERRS spectra. Hence, in our opinion, instead of using the term "doping-induced frequency shifts" in case of SERRS spectra, it is preferable to talk about "doping-induced frequency splitting" of particular vibrations. As a result of this, one can observe the simultaneous presence of normal modes coming from different symmetries.

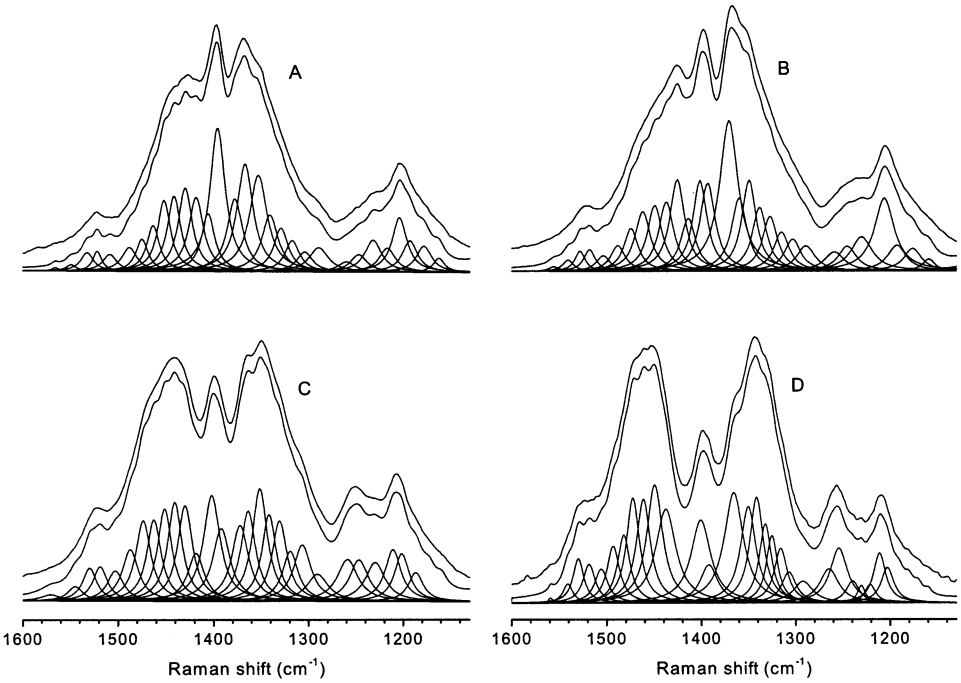

Figure 4. In situ SERRS spectra of P3TOPS on MEA modified Au electrode in 1600−1130 cm^{-1} spectral region at electric potentials applied: −0.3 (A), 0 (B), +0.3 (C), and +0.7 V (D). Deconvolution of the Raman bands into components was made using the same sets of a pure Loretzian lines. From top to bottom of each spectrum: experimental (upshifted for clarity), resolved, and residual spectra.

A good example are the vibrations of the C_α═C_β bond at 1396 cm^{-1}. Upon doping, this polaronic band splits to 1400−1405 cm^{-1} and, at higher doping levels, experiences further splitting to 1438−1461 cm^{-1} which can be assigned mainly to a bipolaronic structure.[56] The modes with highest wavenumbers correspond to the symmetric stretch of the C_α═C_β bond in planar oligothiohenes: α-3T − α-6T structures.[40] Also, at potential applied 0 V (Figure 4B) very intensively start to grow in double bonds region doping-induced symmetric stretches of quinoid-structured C_α═C_β bonds: 1488, 1474 cm^{-1}, and also present ν_s(C_α═C_β) vibrations of planar oligothiophenes[40,41] at 1414 cm^{-1} (bithiophene), 1425, 1450 cm^{-1} (terthiophene), 1461 cm^{-1} (sexithiohene), and also 1437 cm^{-1} (polymethylthiophene of C_s symmetry).

Asymmetric vibrations of the C_α═C_β bonds also display frequency splitting upon doping: the higher frequencies of ν_a-(C_α═C_β) at 1555−1540 cm^{-1} belong to α-2T (C_{2h} symmetry), medium frequencies at 1530−1518 cm^{-1} belong to α-3T (C_{2v} symmetry), whereas the lower frequencies at 1503−1508 cm^{-1} belong to α-6T (C_{2h}).[40] As can be seen, the SERRS spectrum reveals the simultaneous presence of different symmetries and, hence, of differently conjugated chain fragments in doped P3TOPS.

It is known that bipolaron formation is only possible for six-member (α-6T) segments of polythiophene derivatives and longer,[2] i.e., for the longer conjugated chain fragments, whereas the polaron formation is possible only for shorter oligomers. Generally, the vibrations coming from slightly oxidized segments with smaller conjugation length (corresponding to polaron structure) should be enhanced by shorter excitation lines, whereas those from doubly oxidized and longer conjugated segments will be in resonance with longer (λ_{ex} = 676, 781, or 1064 nm) excitation wavelengths.[46,48,56] Therefore, in our case (λ_{ex} = 1064 nm), strong enhancement of bipolaron self-localized excitations is expected.

A question of predominance of polaron and bipolaron structure at different doping levels is still highly debated in the literature.[17,23,70−72,74] The assignment of the RR doping-induced bands is not clear enough, but several efforts have been already made in an attempt to classify them into polaron and bipolaron modes.[46,73−75]

As can be seen from Figures 3 and 4, at low applied potential (up to +0.1 V), the following SERR bands dominate: 1533, 1522, 1440, 1428, 1365, 1304, 1203, 1396, 1400, and 1350 cm^{-1}. The first seven bands are normal vibrational modes of thiophene and oligothiophene. Furukawa[46] has measured the RR spectra of the neutral form, radical cation, and dication of α-6T. The bands at 1330−1350 cm^{-1} were attributed to polaronic structure,[42,46] and the bands at 1419, 1438, 1450, and 1461 cm^{-1} were attributed to the bipolaronic structure[56] of α-6T.

The most intense band in SERRS spectrum at −0.3 V is 1396 cm^{-1}, which is symmetric intra-ring thiophene stretch (C_α═C_β)−H associated with the quinoid structure (polaron band). The second intense band is located at 1367 cm^{-1}, which is assigned to the symmetric intra-ring C_β−C_β stretch (in plane) of the neutral polythiophene.[41,44,46,49] Because the relative intensity of the bands at 1396 and 1419 cm^{-1} increases at lower potentials and decreases at higher potentials, we assign them to polaronic charge carriers, which is also supported by other experimental evidences.[55,65] On the other hand, the bands at 1450, 1304, and 1290 cm^{-1} are most likely bipolaronic.[46]

The energy of the C_α═C_β symmetric stretch vibration in thiophene greatly depends on the symmetry[40,41] (and conjugation length) but the ν_s(C_β−C_β) normal modes of oligo-, PT, and their derivatives are relatively independent of substitution and conjugation at the α position of the thiophene ring.[45] In fully aromatic thiophene rings, they are found[40,41,45,48,49,52,63] at 1370−1365 and 1350 cm^{-1} (for the C_{2h} symmetry) or 1362 and 1314 cm^{-1} (for the C_{2v} symmetry). In polyalkylthiophenes, the normal symmetric C_β−C_β stretch mode is observed[45,48] at 1370−1380 cm^{-1}. Upon oxidation, this ν_s(C_β−C_β) mode experiences only a minor energy shift, and semiquinoid and quinoid C_β═C_β bonds of polyalkylthiophenes exhibit their Raman-active symmetric stretch vibrations[49,63,76,77] at 1376−1380 cm^{-1}. For polyalkox-

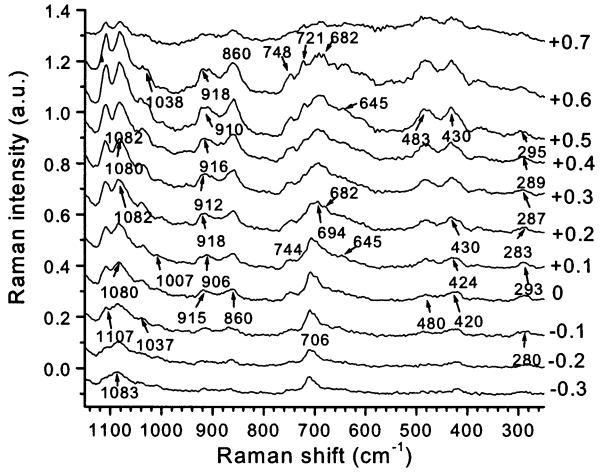

Figure 5. In situ SERRS of P3TOPS on MEA modified Au electrode in 1100−250 cm^{-1} spectral region at different applied electric potentials with excitation 1064 nm. For clarity the spectra are shifted relative to each other.

ythiophenes, these frequencies have been reported at[51] 1300−1305 and 1290−1305 cm^{-1},[46] respectively. The biggest enhancement observed at 1371 cm^{-1} in SERRS spectrum of P3TOPS at 0 V (Figure 4B) and the attribution of the 1362−1367 cm^{-1} line to ν_s(C$_\beta$−C$_\beta$) mode of benzenoid-structured thiophene of C_{2v} symmetry strongly suggest that the 1371 cm^{-1} line belongs to ν_s(C$_\beta$═C$_\beta$) of the quinoid thiophene ring (bipolaron structure).

The bands at 1260−1245 cm^{-1} are assignable to in-plane C$_\beta$−H deformations of the oxidized thiophene ring,[40] and the bands at 1200−1232 cm^{-1} are assignable to the inter-ring C$_\alpha$−C$_{\alpha'}$ stretching vibrations of neutral PT[16,44] and their doping-induced states.[43,46,51]

At +0.2 and +0.3 V (Figure 3), the band at 1304−1306 cm^{-1}, which has been weak at lower potentials, starts to increase in intensity. Its attribution to a polaronic state[46,51,74] is problematic, and it is more likely a bipolaronic band because upon doping the polaronic RR bands at first grow and then decrease, whereas the bipolaronic RR bands increase monotonically.[78]

The evolution of the doping-induced SERRS bands in the 1600−1130 cm^{-1} spectral range can be summarized as follows. At low doping levels (up to 0 V), the polaron bands dominate. Then, at 0 V and +0.1 V, the polaron and bipolaron bands coexist, and at +0.2 V, the bipolaron bands prevail. From +0.2 up to +0.4 V, the polaronic and bipolaronic along with benzenoid-structured segments are all observed but, at the highest doping levels (from +0.5 to +0.7 V), dominate bands assigned to bipolarons and to the benzenoid-structured segments.

3.5.2. Doping-Induced Orientational Changes in P3TOPS. Because a high conductivity of polyconjugated polymers is associated not only with the generation of a high number of charge carriers but mainly with the extension of the conjugation length and planarity, it is of critical importance to obtain upon doping as coplanar a structure of polymer as possible. The orientation of the adsorbate molecules on the electrode surface can be estimated from the enhancement of the relevant SERRS bands by the use of the surface selection rules, which are based on the image dipole theory as predicted by Creighton et al.[79] and developed further by Moskovits.[80,81] In particular, the doping-induced conformational and orientational changes of the thiophene ring on the gold surface upon electrochemical doping can be understood by the relative magnitude of ring deformation vibrations (in-plane δ (C−S−C) vibration at 706 cm^{-1} and δ-(C$_\beta$H) and out-of-plane deformation vibration γ(CH)[40,45] at 645 and 682−701 cm^{-1}; Figure 5).

At 0 V, the amount of chain segments, having C_s point group (coplanar structure of polythiophene),[41,46,56] increases and new bands start to grow at 721 and 744 cm^{-1}. The latter band at 744 cm^{-1} is present in SERRS spectra of P3TOPS even at −0.2 V, it reaches its relative intensity maximum at approximately 0 to +0.1 V and does not grow further. Bazzaoui[68] recently assigned this band to the symmetric stretch of the C−S bond in polyoctylthiophene. Another new band at 721 cm^{-1} starts to develop at +0.2 V, and it also has been observed[40] (although without any interpretations) in RR spectra of chemically doped α-6T with use of laser excitation λ_{exc} = 1064 nm. It is interesting that this transition in similar experiments,[40] but with 457.9 and 514.5 nm excitations, has been absent. It supports the idea that the band at 721 cm^{-1} comes from the bipolaron state of the fully doped 6T-conjugated P3TOPS fragment. The mode at 744 cm^{-1}, in our opinion, corresponds to the polaron charge carrier state with semiquinoid structure of thiophene rings and shorter conjugation length between P3TOPS units.

The out-of-plane or so-called "kink-modes" of thiophene ring at 682, 694, and 645 cm^{-1} start to develop at potentials positive to +0.1 V. These bands were assigned to defects[40] and are considered to be related to the distorted conformation around thiophene inter-ring single bonds in doped polymer.

At potentials above +0.1 V the ring experiences distortions. The "ring breathing" mode (by investigation by the Garreau group, it was assigned to symmetric CS stretch[66]) also experiences an increase in intensity upon doping and a continuous shift in position (915 → 918 → 912 → 916 → 918 cm^{-1}). This also confirms that C−S−C linkage exhibits distortions upon doping.

The C−H and C−O deformation vibrations, according to the surface selection rule, also show structural and orientational changes upon electrochemical oxidation. In fact, the asymmetrically shaped and splitted at higher potentials band at 1130−1050 cm^{-1} consists of several overlapping vibrations of oxidized P3TOPS, including the (COC) antisymmetric stretch at 1068 cm^{-1}, in plane (C$_\beta$−O) and (C$_\beta$−H) deformations[40,45,48,51,56,63,68] at 1082−1090 cm^{-1}, and the stretch mode of COCC linkage at 1107 cm^{-1}. At potentials positive to +0.1 V, because of possible twist between chain fragments with different symmetry, another thiophene δ(C$_\beta$−H) deformation mode[44,45] at 1037 cm^{-1} begins to grow. This implies the formation of chain segments with another conjugation. The band at 1107 cm^{-1}, which also have been observed in Raman spectra of poly(3,3′-dibutoxy-2,2′-bithiophene),[51] belongs to the helical-structured COCC chain[53,54] and starts to grow above 0 V.

The Raman intensity of the out-of-plane γ(CH) ring deformation mode[40] at the vicinity of 906−908 cm^{-1} visibly grows in the potential range between +0.3 and +0.6 V, also indicating the twist of the polymer chain in this potential range.

3.5.3. Role of the Alkoxy Side Chain in Reorientation of P3TOPS Molecule. In connection with these observations, it is interesting to trace the alkoxy side chain orientation of P3TOPS on the gold surface. Generally speaking, ethers tend to exhibit rotational isomerism[39] with Raman modes of the different rotamers being observed at different frequencies. Therefore, it is not surprising that in the SERRS spectra of P3TOPS one can observe several stretching vibrations at 1068, 1007, and 1107 cm^{-1}. The growth of the sharp peak at 1107 cm^{-1} belonging to the (COCC) stretching vibration[48] of a helical highly oriented ether group[54] supports the view that upon doping the side chain becomes more gauche-conformed. The doping-induced intensity

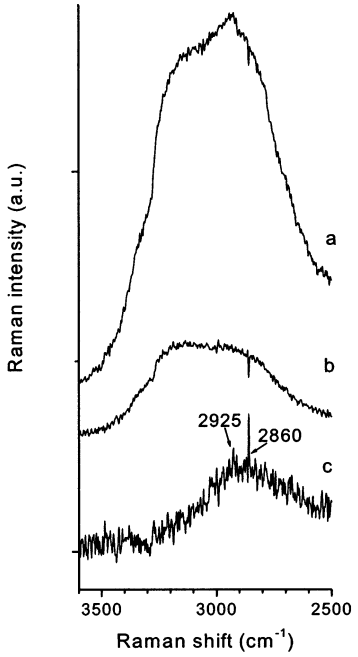

Figure 6. CH-stretching region in SERRS spectra P3TOPS at applied electric potentials +0.5 V (a) and −0.3 V (b), and their differential spectrum (c) obtained after initial normalization of (a) and (b). For clarity, the spectra are shifted relative to each other.

enhancement of the 1107 cm^{-1} line reflects continuous change in the side chain conformation and orientation closer to the surface normal upon doping. Simultaneously, above 0 V, the symmetric deformation vibration δ(COC) at 483 cm^{-1} begins to grow in intensity. It also indicates that the COC group becomes oriented more perpendicular to the gold surface. The red shift toward higher energy with growth in intensity also experiences the symmetrical COCCC deformation mode[39] at 420 cm^{-1}.

As can be seen from Figure 6, in the CH-stretching region upon doping, symmetric and an asymmetric ether CH_2-stretching modes grow at 2860 and 2925 cm^{-1}, respectively, which are characteristic of gauche conformation[82] in the ether group. These observations further confirm that at least in part of the COCCC linkages a trans → gauche conformational change takes place with simultaneous reorientation closer to the surface normal.

From the observations in the 1150−1250 cm^{-1}, spectral range one can conclude that in the potential range from −0.2 to +0.1 V the thiophene rings display the growing coplanarity (i.e., effective conjugation length increases) and show a small inclination against the surface. Above 0 V, the number of alkoxy side chains taking more gauche-like conformations grows, and they become oriented closer to the surface normal. This leads to inevitable distortion in CSC bonds above +0.2 V and to deplanarization of the rings at potentials positive of +0.3 V. These observations are interesting because conformational changes in the side chains of PT derivatives previously were known to induce disorder mainly in the backbone.[83−85]

In light of the results presented above, it is interesting to return to UV−vis spectra of the MEA/P3TOPS multilayer obtained during the electrochemical oxidation in water (our previous publication,[15] Figure 3). The increase of the absorption maximum at the vicinity of 850 nm (1.46 eV) from low to medium doping level ($U \leq +0.3$ V) can be assigned[86,87] to the growing number of polaronic states in PT. After +0.3 V, this band undergoes a red shift until 900 nm (1.38 eV). The same peak has been observed by Fichou et al.[86] as a shoulder of high-intensity band at 1000.6 nm (1.24 eV) which was attributed to $6T^{2+}$ (bipolaronic state) in α-conjugated oligothiophenes. The shift of this band toward longer wavelengths with a simultaneous decrease in absorbance was interpreted as a growing disorder[88] in the polymer chain and as an evidence of polaron delocalization in two dimensions.[23] At +0.3 V, the most intense band is found at 1870 nm (0.66 eV). Upon further oxidation this transition shifts toward higher energy and reaches 1720 nm (0.72 eV) at +0.6 V. It can be interpreted as an evidence of increasing steric strain in the molecule and loss of the planarity due to torsion at the inter-ring bonds. The resulting decrease of the π-conjugation length increases the HOMO−LUMO gap[37,89] and produces a blue shift in the UV−visible spectrum. The behavior of the $\pi \rightarrow \pi^*$ transition band at 630 nm (1.97 eV) also supports this conclusion. At potentials above +0.3 V, it shifts to 625 nm (1.98 eV) with a simultaneous decrease in absorbance, implying the polymer to be partly twisted[85] with the formation of short oligomers.

3.6. SERRS Potential Profiles. As can be seen from Figure 4, the deconvolution of the bands in the SERRS spectra yields clear evidence of nonuniform polaron and bipolaron formation. In principle, the concentration of charge carriers can be determined by the integration of the bands assigned to polarons and bipolarons. However, the overlap of all of the spectral lines situated in the range 1100−1600 cm^{-1} presents a real challenge to spectroscopists trying to use it for any quantitative estimations. Indeed, at low potentials applied, the Raman lines generally exhibit Lorentzian shape, but at higher potentials, upon inevitable introduction of disorder, the lines broaden with an emergence of a Gaussian component.[49] Therefore, we consider the curve fitting results presented in Figure 4 to be instructive in a qualitative sense because they basically reflect the evaluation of peak positions and their relative intensities during oxidation, but their use for quantitative estimations is problematic. Therefore, we simplified the problem by focusing our attention at the SERRS bands in four important spectral regions, namely, 1132−1275, 1275−1379, 1379−1415, and 1415−1513 cm^{-1}. Selecting these ranges, we were guided by the fact that each of them basically represents certain vibrational features in the P3TOPS spectra.

The range 1132−1275 cm^{-1} mainly corresponds to inter-ring thiophene stretchings and reflects changes in the conjugation length of P3TOPS as well as the generation of bipolaronic charge carriers upon doping. The in-plane stretch of the $C_\beta-C_\beta$ bond in the benzenoid and semi-quinoid thiophene ring (1363−1371 cm^{-1}) and its C−H deformation modes at 1350−1330 cm^{-1} are situated in the 1275−1379 cm^{-1} range. The quite narrow range 1379−1415 cm^{-1} contains the polaron bands of the symmetric stretch vibrations $(C_\alpha-C_\beta)-H$ at 1396 and 1401 cm^{-1}. Finally, the range 1415−1513 cm^{-1} represents mainly $(C_\alpha=C_\beta)-H$ and $(C_\alpha=C_\beta)-O$ ring stretching vibrations of the chain segments having various conjugation lengths. Integration of each range for all of the experimental SERRS spectra has been performed. For normalization, the area of each SERRS spectrum in a particular range was divided by the total area under the whole spectral region (1600−1130 cm^{-1}, see Figure 4).

Figure 7 represents the variation of the normalized integrated bands in these four selected ranges as a function of the applied potential. Because resonance enhancement and orientation are properly accounted by normalization, the run of these curves reflects mainly the change in number of differently oxidized molecular segments (and some degradation of the film at the highest potential). Thus, variation of the SERRS bands area in the 1379−1415 cm^{-1} range (curve 1 Figure 7) represents a

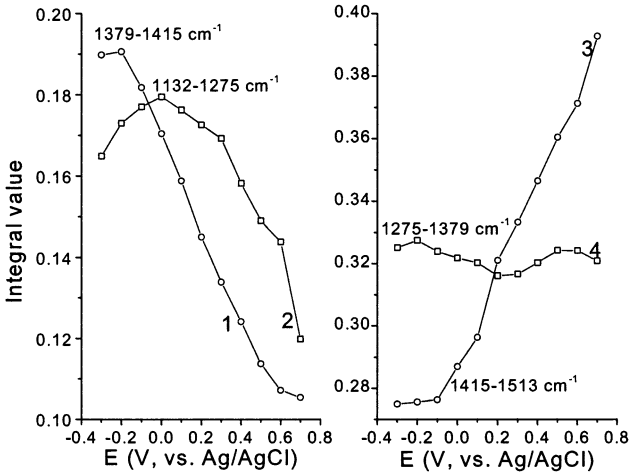

Figure 7. Variation of four normalized integrated spectral ranges in SERRS of P3TOPS as a function of applied electric potential.

monotonic decrease of the polaron band intensities (semi-quinoid structured segments), whereas the area of the bands in the 1415−1513 cm^{-1} range (curve 3) indicates a monotonic increase of bipolarons. It is interesting that the latter curve is not linear. It appears that there are four different potential ranges where the bipolaron bands are formed at a different rate. The lowest rate is observed in the range from −0.3 to −0.1 V, a higher rate between 0 and +0.1 V, and the highest between +0.1 and +0.2 V after which bipolarons appear with constant high rate until the end of the doping process.

From the curve 2 (Figure 7), one can see that below 0 V a substantial growth of the inter-ring double bonds (the increase in conjugation length) is observed. This coincides with the decrease of the neutral and semi-quinoid structural segments in the main chain (left side of curve 4 and curve 1). A further run of curves 2 and 4 appears to be worth discussing.

Wrighton et al.[90−92] have shown that *p*-conductivity of PT and acetylene exhibits a bell-shaped potential dependence and that the highest conduction appears at the current plateau following the main oxidation peak where the polymer film is in the metallic state. The same bell-shaped potential dependence for *p*-conductivity has been observed recently for poly(3.4-ethylenedioxythiophene[93] and poly(3,4-dimethoxythiophene).[4] The bell-shaped conductivity curve for redox conducting polymers has been explained[94,95] by a mixed-valence conduction mechanism, according to which the conductivity is proportional to the neutral, polaronic, and bipolaronic population in polymer chain. The potential dependence observed for normalized integrated SERRS intensities of P3TOPS in the range of inter-ring stretch vibrations (Figure 7, curve 2) also exhibits a bell shape with maximum at 0 V. It is believed that in the potential window between −0.1 and +0.1 V the P3TOPS molecule achieves the largest coplanarity between neighboring polymer units, which is associated with the highest conductivity. At more positive potentials, the conjugation length shortens, and we observe a twist between differently conjugated chain fragments.

4. Conclusions

An electrochemical in situ surface enhanced resonance Raman spectroscopy with excitation at 1064 nm along with UV−visible and resonance Raman spectroscopies are used in order to investigate the dynamic changes between the generation of charge transfer states, structure, and orientation occurring upon oxidative doping of poly-3-(3′thienyloxy)-1-propanesulfonate (P3TOPS) monolayer, self-assembled from aqueous solution on a gold surface modified by 2-mercaptoethylamine (MEA). We demonstrate that at the lower range of potentials applied to the working electrode the planarity of neighboring thiophene rings grows, and at the higher one, it decreases. The analysis of charge-carrier polaron and bipolaron P3TOPS bands in SERRS spectra shows a sequential increase in the generation of bipolaron bands as well as a decrease in the number of polaronic bands upon electrochemical doping.

The potential step shows that upon electrochemical doping until 0 V vs Ag/AgCl the alkoxy side chains of self-assembled P3TOPS exhibit a trans conformation, and we observe a growth in the π-conjugation length with maximum at 0 V. Further oxidation of P3TOPS leads to transformation in part of the side chains to a more gauche-like conformation with simultaneous orientation closer to the surface normal. This conformational change in side chains leads the molecule at potentials positive to +0.2 V to inevitable distortion in thiophene CSC bonds and, at potentials higher than +0.3 V, to the creation of charge defects with further loss of π-conjugation.

Acknowledgment. The financial aid from the Academy of Finland (Grant No. 30579), Turku University Foundation, and also Ella and Georg Ehrnrooth's private foundation is gratefully acknowledged.

References and Notes

(1) *Semiconducting Polymers: Chemistry, Physics and Engineering*; Hadziioannou, G., van Hutten, P. F., Eds.; Wiley−VCH: New York, 1999.
(2) *Handbook of Oligo- and Polythiophenes*; Fichou, D., Ed.; Wiley−VCH: New York, 1998.
(3) Ulman, A. *Chem. Rev.* **1996**, *96*, 1533−1554.
(4) Decher, G.; Schmitt, J. *J. Prog. Colloid Polym. Sci.* **1992**, *89*, 160−164.
(5) Cheung, G. H.; Fou, A. F.; Ferreira, M.; Rubner, M. F. *Polym. Prepr.* **1993**, *34*, 757−758.
(6) Decher, G. *Science* **1997**, *277*, 1232−1237.
(7) Farhat, T. R.; Schlenoff, J. B. *Langmuir* **2001**, *17*, 1184−1192.
(8) McAloney, R. A.; Goh, M. C. *J. Phys. Chem. B* **1999**, *103*, 10729−10732.
(9) Farhat, T.; Yassin, G.; Dubas, S. T.; Schlenoff, J. B. *Lamgmuir* **1999**, *15*, 6621−6623.
(10) Baur, J. W.; Rubner, M. F.; Reinolds, J. R.; Kim, S. *Lamgmuir* **1999**, *15*, 64−69.
(11) Pardo-Yissar, V.; Katz, E.; Lioubashevski, O.; Wilner, I. *Langmuir* **2001**, *17*, 1110−1118.
(12) Villa, E.; Agosti, E.; Castiglioni, C.; Gallazzi, M. C.; Zerbi, G. *J. Chem. Phys.* **1996**, *105*, 9461−9469.
(13) Zotti, G.; Zecchin, S.; Schiavon, G. *Chem. Mater*. **2000**, *12*, 2996−3005.
(14) Lukkari, J.; Viinikanoja, A.; Paukkunen, J., Salomäki, M.; Janhonen, M.; Äätitalo, T.; Kankare, J. *J. Chem. Soc., Chem. Commun.* **2000**, 571−572.
(15) Lukkari, J.; Salomäki, M.; Viinikanoja, A.; Äätitalo, T.; Paukkunen, J.; Kocharova, N.; Kankare, J. *J. Am. Chem. Soc.* **2001**, *123*, 6083−6091.
(16) Wang, R. S.; Wang, L.-M.; Fu, Y.-J.; Su, Z.-M. *Synth. Met.* **1995**, *69*, 713−714.
(17) Yurtsever, E. *Synth. Met.* **1999**, *105*, 179−183.
(18) Wu, C.-G.; Chien, L.-N. *Synth. Met.* **2000**, *110*, 251−255.
(19) Rossi, L.; Lanzani, G.; Garnier, F. *Phys. Rev. B* **1998**, *58*, 6684−6687.
(20) *Introduction to Molecular Electronics*; Petty, M. C., Bruce, M. R., Bloor, D., Eds.; Edward Arnold: London, 1999.
(21) Salzner, U.; Lagowski, J. B.; Pickup, P. G.; Poirier, R. A. *Synth. Met.* **1998**, *96*, 177−189.
(22) Jiang, X. M.; An, C. P.; Österbacka, R.; Vardeny, Z. V. *Synth. Met.* **2001**, *116*, 203−206.
(23) Österbacka, R.; An, C. P.; Jiang, X. M.; Vardeny, Z. V. *Synth. Met.* **2001**, *116*, 317−320.
(24) Kawai, T.; Nakazono, M.; Sugimoto, R.; Yoshino, K. *Synth. Met.* **1993**, *55−57*, 353−358.
(25) Kawai, T.; Nakazono, M.; Yoshino, K. *Synth. Met.* **1995**, *69*, 379−380.
(26) Weaver, M. J.; Zou, S.; Chan, H. Y. H. *Anal. Chem.* **2000**, *1*, 39A−47A.

(27) Wolkow, R. A.; Moskovitz, M. J. *J. Chem. Phys.* **1987**, *87*, 5858−5866.
(28) Cotton, T. M.; Uphaus, R. A.; Möbius, D. *J. Phys. Chem.* **1986**, *90*, 6071−6073.
(29) Tsen, M.; Sun, Li, *Anal. Chim. Acta* **1995**, *307*, 333−340.
(30) Wasileski, S. A.; Zou, S. *J. Appl. Spectrosc.* **2000**, *54*, 761−772.
(31) Zou, S.; Williams, C. T.; Chen, E. K.-Y.; Weaver, M. J. *J. Am. Chem. Soc.* **1998**, *120*, 3811−3812.
(32) Zou, S.; Weaver, M. J. *Anal. Chem.* **1998**, *70*, 2387−2395.
(33) Ye, O.; Fang, J. *J. Phys. Chem. B* **1997**, *101*, 8221−8224.
(34) Kennedy, B. J.; Spaeth, S.; Dickey, M.; Carron, K. T. *J. Phys. Chem. B* **1999**, *103*, 3640−3646.
(35) Chayer, M.; Faid, K.; Leclerc, M. *Chem. Mater.* **1997**, *9*, 2907−2910.
(36) Gao, P.; Gosztola, D.; Leung, L.-W. H.; Weaver, M. *J. Electroanal. Chem.* **1987**, *233*, 211−222.
(37) Frechette, M.; Belletete, M.; Bergeron, J.-I.; Durocher, G.; Leclerc, M. *Macromol. Chem. Phys.* **1997**, *198*, 1709−1722.
(38) Mulazzi, E.; Ripamonti, A.; Godon, C.; Lefrant, S. *Synth. Met.* **1995**, *69*, 671−673.
(39) Dollish, F.; Fately, W. G.; Bently, F. F. *Characteristic Raman Frequencies of Organic Compounds*; Willey: New York, 1974.
(40) Louarn, G.; Buisson, J. P.; Lefrant, S.; Fichou, D. *J. Phys. Chem.* **1995**, *99*, 11399−11404.
(41) Louarn, G.; Mevellec, J. Y.; Buisson, J. P.; Lefrant, S. *Synth. Met.* **1993**, *55*−*57*, 587−592.
(42) Lopez Navarette, J. T.; Zerbi, G. *J. Chem. Phys.* **1991**, *94*, 957−964 and 4161−4170.
(43) Shi, G.; Xu, J.; Fu, M. *J. Phys. Chem. B* **2002**, *106*, 288−292.
(44) Bazzaoui, E. A.; Levi, G.; Aeiyach, S.; Aubard, J.; Marsault, J. P.; Lacase, P. C. *J. Phys. Chem.* **1995**, *99*, 6628−6634.
(45) Louarn, G.; Mevellec, J. Y.; Lefrant, S.; Buisson, J. P.; Fichou, D.; Teulade-Fichou, M. P. *Synth. Met.* **1995**, *69*, 351−352.
(46) Furukawa, Y. *J. Phys. Chem.* **1996**, *100*, 15644−15653.
(47) Luzny, W.; Pron, A. *Synth. Met.* **1995**, *69*, 337−338.
(48) Louarn, G.; Trznadel, M.; Buisson, J. P.; Laska, J.; Pron, A.; Lapkowski, M.; Lefrant, S. *J. Phys. Chem.* **1996**, *100*, 12532−12539.
(49) Lefrant, S.; Baltog, I.; de la Chalelle, M. L.; Baibarac, M.; Louarn, G.; Journet, C.; Bernier, P. *Synth. Met.* **1999**, *100*, 13−27.
(50) Louarn, G.; Trznadel, M.; Zagorska, M.; Lapkowski, M.; Pron, A.; Buisson, J. P. *Synth. Met.* **1997**, *84*, 579−580.
(51) Pron, A.; Louarn, G.; Lapkowski, M.; Zagorska, M.; Glowczyk-Zubek, J.; Lefrant, S. *Macromolecules* **1995**, *28*, 4644−4649.
(52) Costa-Bizzari, P.; Della-Casa, C.; Lanzi, M.; Bertinelli, F.; Iarossi, D.; Mucci, A.; Schenetti, L. *Synth. Met.* **1999**, *104*, 1−7.
(53) Valiokas, R.; Svedhem, S.; Svensson, S. C. T.; Liedberg, B. *Langmuir* **1999**, *15*, 3390−3394.
(54) Valiokas, R.; Östblom, M.; Svedhem, S.; Svensson, S. C. T.; Liedberg, B. *J. Phys. Chem. B* **2000**, *104*, 7565−7569.
(55) Kunath, D. *Chem. Ber.* **1963**, *96*, 157−159. Ohno, K.; Naganobu, T.; Matsuura, H. *J. Phys. Chem.* **1995**, *99*, 8477−8484.
(56) Garreau, S.; Louarn, G.; Buisson, J. P.; Froyer, G.; Lefrant, S. *Macromolecules*, **1999**, *32*, 6807−6812.
(57) Casado, J.; Maraver Puig, J. J.; Hernandez, V.; Zotti, G.; Lopez Navarette, J. T. *J. Phys. Chem. A* **2000**, *104*, 10656−10661.
(58) Winokur, M. J.; Walmsley, P.; Moulton, J.; Smith, P.; Heeger, A. J. *Macromolecules* **1991**, *24*, 3812−3816.
(59) Prosa, T. J.; Winokur, M. J.; Moulton, J.; Smith, P.; Heeger, A. J. *Macromolecules* **1992**, *25*, 4364−4369.
(60) Prosa, T. J.; Winokur, M. J.; Moulton, J.; Smith, P.; Heeger, A. J. *Synth. Met.* **1993**, *55*, 370−377.
(61) Shimoi, Y.; Abe, S. *Synth. Met.* **1995**, *69*, 687−688.
(62) Magela e Silva, G.; Ono, Y. *Synth. Met.* **1998**, *97*, 195−203.
(63) Garreau, S.; Louarn, G.; Froyer, G.; Lapkowski, M.; Chauvet, O. *Electrochim. Acta* **2001**, *46*, 1207−1214.
(64) Kudelski, A.; Kryznski, P. *J. Electroanal. Chem.* **1998**, *443*, 5−7.
(65) Lanzani, G.; Nisoli, M.; De Silvestri, D.; Tubino, R. *Chem. Phys. Lett.* **1996**, *251*, 5−6, 339−345.
(66) Garreau, S.; Duvail, J. L.; Louarn, G. *Synth. Met.* **2002**, *125*, 325−329.
(67) Cho, S. I.; Park, E. S.; Kim, K.; Kim, M. S. *J. Mol. Stuct.* **1999**, *479*, 83−92.
(68) Bazzaoui, El. A.; Bazzaoui, M.; Aubard, J.; Lomas, J. S.; Felidj, N. G.; Levi, G. *Synth. Met.* **2001**, *123*, 299−309.
(69) Tran-Van, F.; Garreau, S.; Louarn, G.; Froyer, G.; Chevrot, C. *J. Mater. Chem.* **2001**, *11*, 1378−1382.
(70) Pemberton, J. E. In *Electrochemical Interfaces: Modern Techniques for in-situ interface characterization*; Abrunä, H. D., Ed.; VCH: New York, 1991.
(71) Emin, D. *Phys. Rev.* **2000**, *61*, 6069−6085.
(72) Magela e Silva, G. *Phys. Rev. B* **2000**, *61*, 10777−10781.
(73) Sakamoto, A.; Furukawa, Y.; Tasumi, M. *J. Phys. Chem.* **1992**, *96*, 3870−3874.
(74) Furukawa, Y. *Synth. Met.* **1992**, *49*−*50*, 335−340.
(75) Veronelli, M.; Gallazzi, M.; Zerbi, G. *Synth. Met.* **1993**, *55*−*57*, 545−551.
(76) Meille, S. V.; Farina, A.; Bezicheri, F.; Gallazzi, M. C. *Adv. Mater.* **1994**, *6*, 848−851.
(77) Wang, J.; Zou, B.; Hong, X.; Collard, D. M. *Synth. Met.* **2000**, *113*, 223−226.
(78) Orion, I.; Buisson, J. P.; Lefrant, S. *Phys. Rev. B* **1998**, *57*, 7050−7065.
(79) Creighton, J. A.; Blatchford, C. G.; Albrecht, M. G. *J. Chem. Soc., Faraday Trans.* **1979**, *75*, 790−798.
(80) Moscovits, M.; Suh, J. S. *J. Phys. Chem.* **1984**, *88*, 5526−5530.
(81) Moscovits, M.; Suh, J. S. *J. Phys. Chem.* **1988**, *92*, 6327−6329.
(82) Harder, P.; Grunze, M.; Dahint, R.; Whitesides, G. M.; Laibins, P. E. *J. Phys. Chem. B* **1998**, *102*, 426−436.
(83) Meille, S. V.; Farina, A.; Bezicheri, F.; Gallazzi, M. C. *Adv. Mater.* **1994**, *6*, 848−851.
(84) Tashiro, K.; Kobayashi, M.; Morita, S.; Yoshino, K. *Synth. Met.* **1995**, *69*, 397−398.
(85) Levesque, I.; Leclerc, M. *Synth. Met.* **1997**, *84*, 203−204.
(86) Fichou, D.; Horovitz, G.; Xu, B.; Garnier, F. *Synth. Met.* **1990**, *39*, 243−259.
(87) Furukawa, Y. *Synth. Met.* **1995**, *69*, 629−632.
(88) Schreiber, M.; Abe, S. *Synth. Met.* **1993**, *55*−*57*, 50−55.
(89) Corish, J.; Feeley, D. E.; Morton-Blake, D. A. *J. Phys. Chem. B* **1997**, *101*, 10075−10085.
(90) Ofer, D.; Wrighton, M. S. *J. Am. Chem. Soc.* **1988**, *110*, 4467−4468.
(91) Crooks, R. M.; Chyan, O. M.; Wrighton, M. S. *Chem. Mater.* **1989**, *1*, 2−10.
(92) Ofer, D.; Park, L. Y.; Schrock, R. R.; Wrighton, M. S. *Chem. Mater.* **1991**, *3*, 573−578.
(93) Ahonen, H. J.; Lukkari, J.; Kankare, J. *Macromolecules* **2000**, *33*, 6787−6793.
(94) Zotti, Z.; Schiavon, G. *Chem. Mater.* **1991**, *3*, 62−65.
(95) Faid, K.; Leclerc, M.; Nguyen, M.; Diaz, A. *Macromolecules* **1995**, *28*, 284−287.